TRANSIENT RESPONSE OF CAPACITIVE VOLTAGE TRANSFORMERS

by

Dr. J.R. Lucas and

P.G. McLaren

Keywords :- C V T, Voltage transformer, ferro-resonance, saturation, computer simulation

Abstract

The paper presents an accurate model for representing Voltage Transformers and Capacitive Voltage Transformers in transient studies. The magnetising characteristic of the transformer is based on the non-linear power curve representation [1]. Subharmonic oscillations during short circuit faults in the primary system, which cause relaying problems, and Ferro-resonance behaviour after fault clearance including its suppression, have been successfully simulated by the model. The results are seen to agree with reported investigations [2,3,4].

List of Principal Symbols

C_1, C_2	- capacitance elements of divider
i	- total exciting current injected at core
i_c	- core loss component of exciting current
i_m	- magnetising component of current
I_{eq}, R_{eq}	- Dommel's equivalent elements
l_p, r_p	- primary inductance and resistance of VT
l_s, r_s	- secondary inductance & resistance of VT
L	- Compensating inductance
n	- turns ratio
n	- suffix n, integral time (t/Δt)
S_n	- estimate of 'reluctance' (based on flux linkage, rather than on flux)
S_n	- corrected value of 'reluctance' of core
t	- instant of time
Δt	- time step used in simulation
v_{in}	- estimate of core voltage from EMTDC simulation
v_n	- corrected value of core voltage
$v_{th,n}$	- Thevenin's voltage at core due to rest of VT circuit
z_{th}	- Thevenin's equivalent impedance of rest of VT circuit (Dommel's equivalent)
k_i	- coefficients of power curve expansion
α_i	- indices of power curve expansion
ϕ	- core flux linkage
C_f	- Suppression filter capacitance
L_f	- Suppression filter inductance
r_f	- resistance of filter inductor
R_f	- Suppression filter resistance
R_s, X_s	- series elements of ANSI Standard Burden
R_p	- parallel element of ANSI Burden

1.0 Introduction

An accurate model for representing the Voltage Transformer (VT) and Capacitive Voltage Transformer (CVT) in transient studies has been formulated. The magnetising characteristic of the voltage transformer in each is based on the non-linear power curve representation [1]. Subharmonic oscillations during short circuit faults in the primary system, which cause relaying problems, and Ferro-resonance behaviour after fault clearance including its suppression, have been successfully simulated by the model. The results of the model agree with reported investigations [2,3,4].

The CVT is dealt with in more detail in the following sections as it is the more complex of the two and also incorporates a VT in its design.

CVTs have been used successfully for many years as input devices to electromechanical, and more recently to digital relays. These transform the transmission voltages to designated low voltages through a sequence of a capacitive potential divider and a voltage transformer. The voltage finally available to the protective relay should ideally be an exact replica

Dr. J.R. Lucas is an Associate Professor in Electrical Engineering at the University of Moratuwa, Sri Lanka, and is the Head of its Division of Power Systems and High Voltage Engineering. He obtained his BSc Engineering degree from the University of Ceylon, Peradeniya in 1969. His PhD is in the area of Power System Transient Analysis. He is a Fellow of both the IEE and the IESL and a Chartered Engineer.

Dr. P.G. McLaren is the NSERC Industrial Research Chair in Power Systems at the University of Manitoba, Canada. He obtained his Bachelor's degree from the University of St. Andrews, Scotland in 1958. His PhD is in the area of Power System Protection. He is a Professional Engineer in the Province of Manitoba, a Senior Member of the IEEE and a Chartered Engineer in Europe.

of the transmission voltage. However, when the burden is an electro-mechanical relay, a relatively heavy current is drawn from the protective device and a large error could result. Thus for better accuracy, the loading effect on the capacitive divider is tuned, during normal operation at power frequency, by a compensating reactor on the primary side of the voltage transformer. However, small errors would still be present due to the magnetising current and the secondary impedance of the transformer. Figure 1 shows a schematic diagram of the arrangement [2].

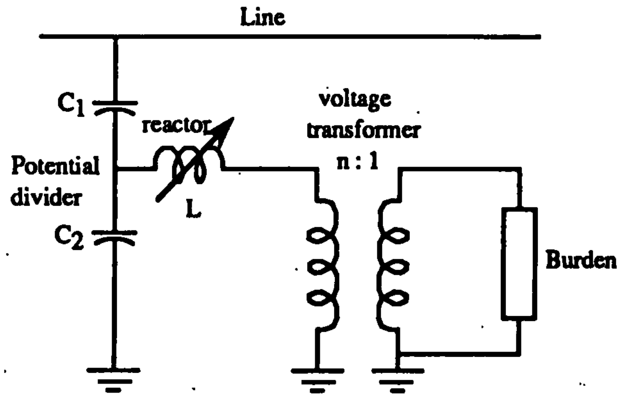

Figure 1 - Schematic diagram of CVT

If the exact burden is known, the reactor could even be slightly detuned to give a higher accuracy for a particular burden [2].

2.0 Transient Response of CVTs

An important area in the design of modern Capacitive Voltage Transformers is its response to transient conditions. Sudden voltage changes, either in the primary system or the secondary system could cause ferro-resonance in the CVT, especially when starting from a previously magnetised state, and dependent on the point-on-wave at which switching occurs. A system which is composed of capacitors and iron-cored inductances is subject to possible ferro-resonant oscillations [5], because of the possibility of the capacitor resonating with a particular value of the non-linear inductance. These ferro-resonant oscillations may either be sustained power frequency oscillations or subharmonic oscillations occuring at a submultiple of the supply frequency [3].

During a fault, the fidelity of the response of the CVT is important for the relay to operate properly. Thus ferro-resonance suppression devices are normally included in the CVT. This ferro-resonance suppression may be "active" or "passive" depending on whether the suppression device stores energy and affects the inherent response of the CVT or not. For example, a permanently connected loading resistor across the voltage transformer output could be used as a "passive" device. However, to be sufficiently effective, its loading would severely reduce the accuracy of the measuring system. On the other hand a suppression device which contains inductors and capacitors would be "active" as these components are energy storing devices and can have a significant effect on the response time unless carefully designed. However, these may be tuned such that under normal power frequency conditions the accuracy is not affected. Figure 2 shows the inclusion of such an "active" ferro-resonant suppression system [4].

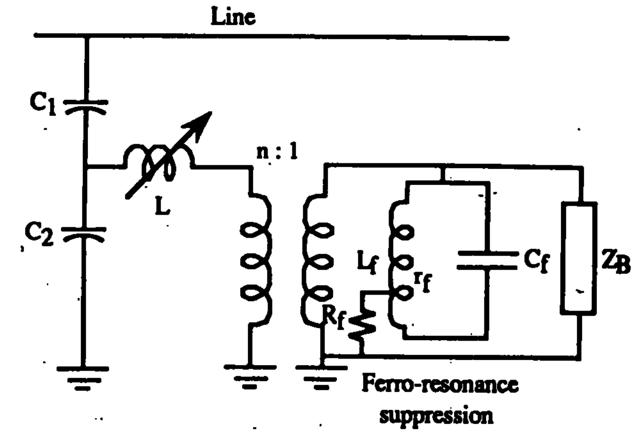

Figure 2 - CVT incorporating ferroresonant suppression

3.0 Simulation of the CVT

In the present study, the transient simulation of the CVT has been carried out with all quantities referred to one side of the voltage transformer for convenience. All the components in the network other than the magnetisation characteristic of the transformer and its coreloss are simulated using a Dommel type analysis [6] on the Manitoba HVDC Research Centre's EMTDC package [7]. The transformer magnetisation characteristic has been simulated based on the approach of Lucas [1], where the magnetising current is expressed as a power series of flux, as given in equation (1).

$$i_m = \Sigma k_i \, \Phi^{\alpha_i} \qquad (1)$$

where k_i are all chosen to be positive coefficients and the indices α_i are also chosen to be positive but not necessarily integers. If the ankle region needs to be represented accurately, index would have a value of less than unity, otherwise this could be conveniently chosen as unity. Typically 3 terms of the power curve give a very good representation over a very wide range of values.

The hysterisis loss has been modelled as a non-linear function of voltage and the eddy current loss as a shunt resistor. The core loss current i_c can thus typically be represented in the form given in equation (2). An additional term may be sometimes added to represent the losses in the saturated region.

$$i_c = c_1 v^{\beta} + \frac{v^2}{R} \qquad (2)$$

The transformer exciting current excluding the eddy current component (i.e. magnetising current and hysterisis loss current) is injected into the model at each instant. The hysterisis phenomenon is not represented by elements of a conductance matrix, as is the case in many EMTP studies.

The burden selected for the CVT in the study is the ANSI standard burden [3], which consists of a pure resistance of R_P in parallel with an impedance (R_s, X_s) having a lagging power factor of 0.5.

3.1 Computation of injected current

Under normal operating conditions, the change in exciting current injected from time step to time step is small so that it may be injected directly as a current source at the next instant without any significant error. However, once saturation is reached the magnetising component of the injected current would be large causing the voltage at the core, from which the current is calculated to change significantly. This change would cause the current injected to be different as well. Under this condition a direct computation of the current to be injected is no longer valid. Thus in the present model, a Thevenin's equivalent of the Dommel's equivalent resistances of the rest of the VT circuit are included in determining the injected current.

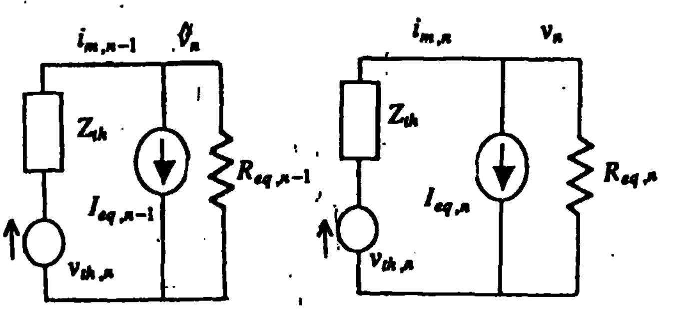

(a) for estimated $\hat{v}_n$ (b) for corrected v_n

Figure 3 - Thevenin's equivalent using Dommel's impedances

Figure 3 shows the Thevenin's equivalent circuit used in determining the magnetising current and hysterisis loss current to be injected into the EMTDC simulation at the next time instant.

The voltage at the VT core $\hat{v}_n$ is estimated from the EMTDC simulation with the magnetising current injection based on an estimate of the flux (figure 3a).

The actual core voltage v_n on the other hand would occur when the rest of the circuit remains unchanged (i.e. the same Thevenin's equivalent) but the magnetising current has the present value (figure 3b).

It can be shown (Appendix A1) that this voltage v_n can be expressed in terms of the estimates of voltage ($\hat{v}_n$), reluctance of core ($\hat{S}_n$). Thevenin's impedance Z and the earlier values of flux ($\Phi_{n-\frac{1}{2}}$), and current ($i_{m,n-1}$) as in equation (3).

$$v_n = [\hat{v}_n - (\hat{S}_n(\Phi_{n-\frac{1}{2}} - i_{m,n-1}).Z_{th}]/(1+Z_{th}.\hat{S}_n.\frac{\Delta t}{2}) \quad (3)$$

The values of reluctance, flux, and current are then updated as follows for use in the evaluation at the next instant.

The actual flux Φ_n, at the present instant is now given as in equation (4).

$$\Phi_n = \Phi_{n-\frac{1}{2}} + v_n . \frac{\Delta t}{2} \quad (4)$$

and the actual reluctance as in equation (5).

$$S_n = f(\Phi_n) \quad (5)$$

Thus the magnetising current at the present instant is given as in equation (6).

$$i_{m,n} = S_n . \Phi_n \quad (6)$$

The hysterisis current is now determined as a function of as in equation (7).

$$i_{c,n} = f_c(v_n) \quad (7)$$

The total exciting current is now obtained as in equation (8).

$$i_n = i_{m,n} + i_{c,n} \quad (8)$$

Finally the flux-linkage at the next mid-interval is determined as in equation (9).

$$\Phi_{n+\frac{1}{2}} = \Phi_n + v_n . \frac{\Delta t}{2} \quad (9)$$

The equivalent circuit beyond the compensating reactor is simulated in the transient study as given in figure 4, with all quantities referred to the primary side.

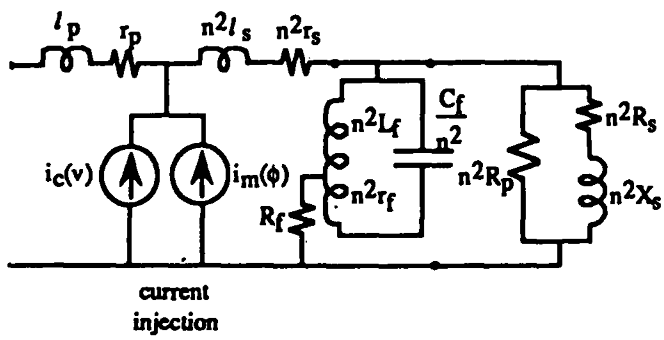

Figure 4 - Equivalent circuit in the simulation

4.0 Results

A fault study was carried out using the model developed to monitor the primary voltage. Since practical Capacitive Voltage transformers are known to develop a residual voltage of the subharmonic oscillation type during short circuit faults in the primary system, this situation was first simulated.

The burden selected for the tests was a typical 200 VA burden with power factors in the range 0.7 lag to unity. The data selected for the CVTs was based on those used at the Dorsey Station in the Manitoba Hydro System on the 500 kV line to Minnesota. [vide: Appendix A2)

Figure 5 shows the input and output voltage waveforms for a unity power factor burden with fault initiation at a voltage zero.

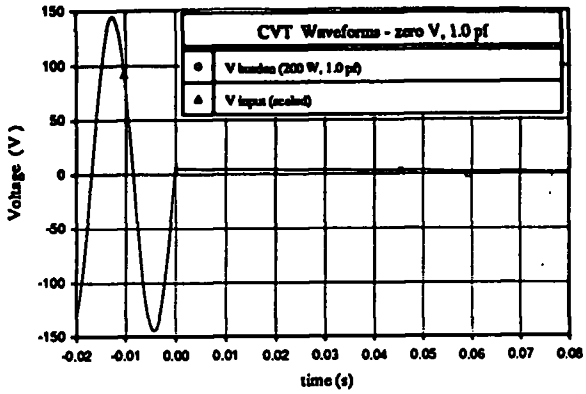

Figure 5 - Voltage waveforms at zero initiation, p.f. = 1.0

A small residual decaying voltage is seen on the burden waveform, which is of course zero in the input waveform. This is known to be the case in practice (2).

Figure 6 shows the same waveforms for a 0.7 lagging power factor ANSI standard burden. This figure shows the decaying residual for the unity power factor case changing to a unidirectional residual. This is again as reported (4).

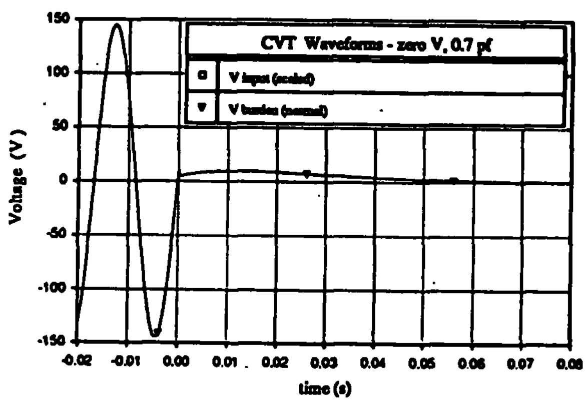

Figure 6 - Voltage waveforms at zero initiation, p.f. = 0.7

The behaviour of the CVT with a 0.7 lagging burden was investigated for the case of the voltage transformer with a significantly higher magnetising current. The amplitude and the frequency of the low frequency oscillations of the residual voltage increased with reducing the power factor as seen in figure 7. This again is typical of reported investigations.

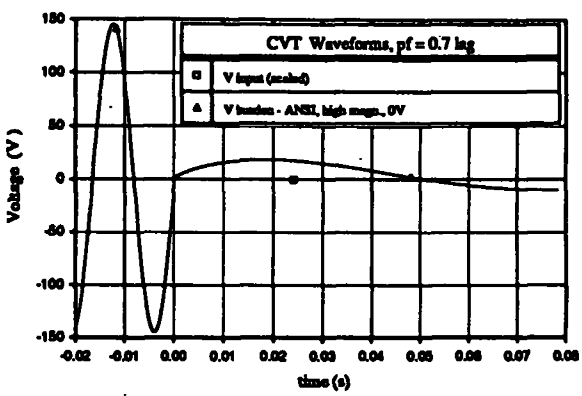

Figure 7 - Voltage waveforms at zero initiation, p.f. = 0.7 high magnetising current

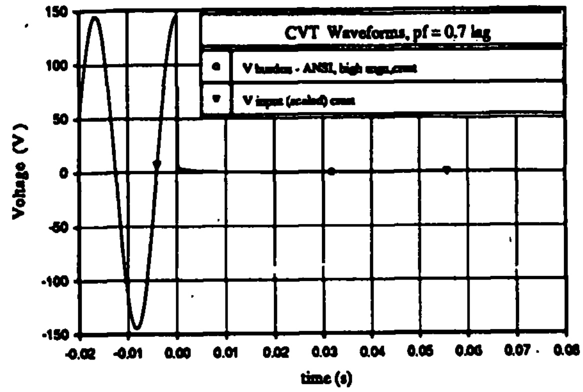

Figure 8 - Voltage waveforms at crest initiation, p.f. = 0.7

The investigation was repeated with fault initiation at voltage crest with the higher magnetising current. The residual voltages are seen to be reduced in magnitude as expected as this occurs at a flux zero, and also in agreement with reported investigations. Figure 8 shows the result.

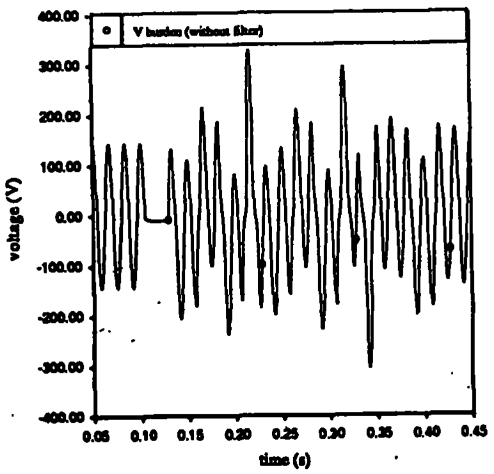

Figure 9a - Voltage waveforms of CVT showing ferroresonance

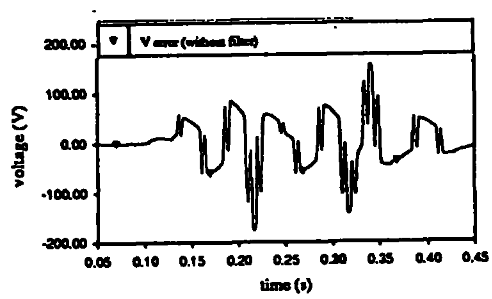

Figure 9b - Error Voltage waveforms of CVT

The next change in the verification of the model was the simulation of the fault clearance and the observation of any ferro-resonance behaviour. A particularly severe condition was selected where the fault occurred at a flux peak and was cleared soon after at a flux peak of cleared waveform. A very low burden was also considered to give negligible damping. Figure 9a shows the voltage waveform, where the fault was initiated at 0.1s and cleared at 0.125s (one and a half cycles later). The corresponding error voltage between the scaled input and the output is shown in figure 9b. Ferro-resonance is clearly seen on the waveforms, starting to die only towards the end of the period of observation. This behaviour is also typical of CVTs (4).

A suppression circuit of the form included in figure 2 was then introduced into the circuit. The ferro-resonance is seen to be quickly suppressed (figure 10a & 10b). This behaviour too is typical of the suppression circuits (4).

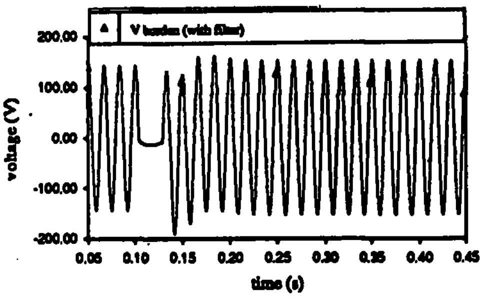

Figure 10a - Voltage waveforms of CVT with ferroresonance suppression

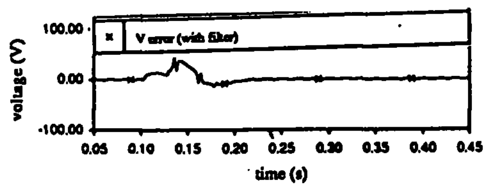

Figure 10b - Error Voltage waveforms of CVT with suppression

5.0 Conclusions

It is seen that the model developed for the Capacitive voltage transformer behaves as expected, both under normal conditions, fault conditions and fault clearance. The method developed is a non-iterative technique and may be implemented into transient solution packages for protection studies.

6.0 References

1. Lucas, J.R., "Representation of magnetisation curves over a wide region using a non-integer power series", IJEEE, Vol. 25, No. 4, 1988, Manchester U.P., UK., pp 335-340.

2. Sweetana, A., "Transient response characteristics of capacitive potential devices", IEEE Trans on PAS, vol PAS-90, Sept/Oct 1971, pp 1989-2001.

3. "Transient response of coupling capacitor voltage transformers IEEE Committee Report", IEEE Trans on PAS, Vol PAS-100, No. 12, Dec 1981, pp 4811-4814.

4. Sweetana, A., and Flugum, R.W., "A new metering accuracy capacitive potential device", IEEE Trans on PAS, Vol PAS-85, No 5, May 1966, pp 499-510.

5. Swift, G.W., "An Analytical approach to ferroresonance", IEEE Trans on PAS, Vol PAS-88, No 1, Jan 1969, pp 42-46.

6. Dommel, H.W., "Digital computer solution of electromagnetic transients in single and multiphase networks", IEEE Trans on PAS, PAS-88, No 4, April 1969, pp 388-399.

7. EMTDC User's Manual, Manitoba HVDC Research Centre, November 1988.

8. Lucas, J.R., and McLaren, P.G., "Simulation of B-H Excursions for Transient Studies", Paper 3, Session MPR7 - Power System II, 33rd Midwest Symposium on Circuits and Systems, Calgary, August 13 1990.

Appendix A1 - Determination of Core Voltage from EMTDC Estimate

Consider figure 3. If the VT circuit, other than the magnetising branch, has a Thevenin's impedance (Dommel's equivalent) of Z_{th} and a Thevenin's voltage source of $v_{th,n}$ at a given instant (figure 3a), then the core voltage estimate $\hat{v}_n$, based on the magnetising current $i_{m,n-1}$ at the previous instant, would be given by equation (A1.1).

$$\hat{v}_n = v_{th,n} - Z_{th} \cdot i_{m,n-1} \qquad \text{(A1.1)}$$

The actual core voltage v_n on the other hand would occur when the rest of the circuit remains unchanged (i.e. has the same Thevenin's equivalent) but the magnetising current has the present value $i_{m,n}$, as in figure 3b, and would be given by equation (A1.2).

$$v_n = v_{th,n} - Z_{th} \cdot i_{m,n} \qquad \text{(A1.2)}$$

Since the Thevenin's equivalent source voltage is not actually known, this is eliminated from equations (A1.1) and (A1.2) to give the actual core voltage in terms of the value from the simulation as given in equation (A1.3).

$$v_n = \hat{v}_n + Z_{th} \cdot i_{m,n-1} - Z_{th} \cdot i_{m,n} \qquad \text{(A1.3)}$$

From the flux-linkage Φ_{n-1} of the previous instant, the flux at the previous mid-interval $\Phi_{n-\frac{1}{2}}$ is known as given in equation (A1.4).

$$\Phi_{n-\frac{1}{2}} = \Phi_{n-1} + v_{n-1} \cdot \frac{\Delta t}{2} \qquad \text{(A1.4)}$$

The flux-linkage $\hat{\Phi}_n$ at the present instant is estimated as in equation (A1.5).

$$\hat{\Phi}_n = \Phi_{n-\frac{1}{2}} + \hat{v}_n \cdot \frac{\Delta t}{2} \qquad \text{(A1.5)}$$

The 'reluctance' $\hat{S}_n$ (based on flux linkage rather than on flux) may be estimated from the power curve representation [1] of the magnetisation characteristic (equation (A1.6)).

$$\hat{S}_n = f(\hat{\Phi}_n) \qquad \text{(A1.6)}$$

The estimated magnetising current $\hat{i}_{m,n}$ at the present instant may be expressed using the reluctance $\hat{S}_n$ in terms of the actual flux as in equation (A1.7).

$$\hat{i}_{m,n} = \hat{S}_n (\Phi_{n-\frac{1}{2}} + v_n \cdot \frac{\Delta t}{2}) \qquad \text{(A1.7)}$$

Thus equation (A1.3) may be rewritten as

$$v_n = \hat{v}_n + Z_{th} \cdot i_{m,n-1} - Z_{th} \cdot \hat{S}_n (\Phi_{n-\frac{1}{2}} + v_n \cdot \frac{\Delta t}{2})$$

which may be simplified to

$$v_n \cdot (1 + Z_{th} \cdot \hat{S}_n \cdot \frac{\Delta t}{2}) = \hat{v}_n - (\hat{S}_n (\Phi_{n-\frac{1}{2}} - i_{m,n-1}) \cdot Z_{th})$$

giving the expression (A1.8)

$$v_n = [\hat{v}_n - (\hat{S}_n (\Phi_{n-\frac{1}{2}} - i_{m,n-1}) \cdot Z_{th}] \; / (1 + Z_{th} \cdot \hat{S}_n \cdot \frac{\Delta t}{2}) \qquad \text{(A1.8)}$$

A modified form of the above algorithm is used when initial remanence is present [8].

Appendix A2 - Principle Data for CVT & Suppression Circuit

CVT ratio	=	4500 : 1
Divider Capacitance C_1	=	0. 116 nF
Divider Capacitance C_2	=	2. 88 nF
Compensating inductance	=	0. 20 H
Voltage transformer primary	=	11. 2 kV
Voltage transformer secondary	=	115. V
Suppression filter capacitance	=	8. μF
Suppression filter inductance rating (60Hz, 115V)	=	230. VA
Suppression filter resistance	=	40. Ω